^{13}C nuclear magnetic resonance and electron spin resonance of amorphous hydrogenated carbon

1998 J. Phys.: Condens. Matter 10 6813

(http://iopscience.iop.org/0953-8984/10/30/019)

J. Phys.: Condens. Matter **10** (1998) 6813–6824. Printed in the UK PII: S0953-8984(98)86937-3

^{13}C nuclear magnetic resonance and electron spin resonance of amorphous hydrogenated carbon

R Blinc†, D Arčon†, P Cevc†, I Pocsik‡, M Koos‡, Z Trontelj§ and Z Jagličič§

† Josef Stefan Institute, Jamova 39, 1000 Ljubljana, Slovenia
‡ Research Institute for Solid State Physics, Budapest, Hungary
§ Institute of Mathematics and Physics, University of Ljubljana, Ljubljana, Slovenia

Received 13 August 1997, in final form 17 April 1998

Abstract. The temperature dependences of the ^{13}C and ^{1}H magnetization recovery and spin–lattice relaxation times as well as the ^{13}C NMR spectra have been studied between 300 K and 4 K. The observed short and nearly temperature independent proton and ^{13}C spin–lattice relaxation times demonstrate that the dominant spin–lattice relaxation mechanism is spin diffusion to paramagnetic impurities. The fact that the magnetization recovery curves clearly deviate from the single-exponential form expected for the case of spin diffusion and randomly distributed paramagnetic centres demonstrates that the paramagnetic centres aggregate in clusters. Superparamagnetic freezing effects expected for such an inhomogeneous distribution are indeed seen below 50 K in the temperature dependence of the electron spin-resonance (ESR) intensity, the ^{13}C NMR spectra and the SQUID magnetization measurements which show a distinct magnetic hysteresis loop.

1. Introduction

The microscopic nature of hydrogenated amorphous carbon (a-C:H) has been recently the subject of intensive study [1–6], but many questions remain open. It has been shown that, by tailoring the deposition conditions [2], a-C:H films can be prepared in such a way that they are harder, denser and more resistant to chemical attack than any other solid hydrocarbon. Together with a high degree of transparency in the infrared and ultraviolet, the above properties of this 'diamond-like amorphous carbon' have led to many applications [1, 2]. In view of its high surface-to-volume ratio, this system represents a nanometric 'surface solid'.

Reliable structural models relating the 'bulk' properties to the structure on an atomic level are, however, still at the stage of development [7–9]. It has been recently suggested that the system is heterogeneous on a nanometric scale and consists of hydrogenated and non-hydrogenated carbons [5]. The proton magnetization recovery could be described in terms of a bi-exponential approach to equilibrium, yielding two time constants whose values are $T_{1a} = 120$ ms and $T_{1b} = 14$ ms at room temperature and at a Larmor frequency of 300 MHz. This result has been interpreted in terms of the existence of two different types of proton cluster spatially separated from each other. The short T_1-component has been attributed [5, 10] to CH groups statistically distributed in the sp^2 and sp^3 carbon network whereas the long T_1-component has been ascribed [5, 10] to short $–CH_2$ polymer-like chain units with an sp^3 configuration. It is proposed that the two groups are separated by 'layers'

0953-8984/98/306813+12$19.50

of non-protonated sp^2 carbons. The intermediate layer should be so large that spin diffusion between the two groups of protons is not effective. The total hydrogen content of such a sample would be 35 at.%.

The mechanism leading to the observed proton spin–lattice relaxation behaviour is however still not fully explained. The absolute values of the two T_1-components as well as their temperature dependences are hard to understand in terms of the relaxation mechanisms normally operating in non-magnetic polymers and organic solids. The rather small value of the shorter T_1-component (5–15 ms) and its near temperature independence cannot be explained in terms of proton–proton dipolar interactions. This is particularly true as the proton density in the sp^2–sp^3 carbon cluster is relatively low and one would in fact expect a long T_1-value rather than such a short one.

To throw some additional light on the structure and magnetic properties of this system, we decided to study the temperature dependence of the ^{13}C and ^{1}H magnetization recovery, the spin–lattice relaxation rates and the ^{13}C NMR spectra. We wanted to see whether the ^{13}C spin–lattice relaxation times show a similarly anomalous behaviour to the proton ones. We also hoped to determine the nature of the mechanism giving rise to the anomalously short proton and ^{13}C T_1-values in a-C:H. Within the two-proton cluster model used to interpret the proton spin–lattice magnetization recovery results, we would expect a three-cluster behaviour in the ^{13}C spin–lattice magnetization recovery. Two ^{13}C clusters would correspond to the two types of protonated carbon cluster and one to the unprotonated carbon layer separating the two proton clusters. Since the ^{13}C nuclei are normally relaxed by C–H dipolar interactions and ^{13}C chemical shift anisotropy fluctuations, the ^{13}C T_1-value of the unprotonated layer should be significantly longer than the T_1-value of the ^{13}C nuclei in the two protonated regions. Two-dimensional (2D) separation-of-interactions ^{13}C NMR spectroscopy was used to determine the inhomogeneous width of the ^{13}C NMR spectra. The 2D ^{13}C separation-of-interactions NMR experiment was repeated at 20 K and 6 K to check on the possible electronic contribution to the inhomogeneous width of the ^{13}C NMR spectra. The electron spin-resonance (ESR) spectra and the static magnetic properties were also studied. SQUID magnetization measurements were used to check on the possible existence of a hysteresis loop at low temperatures.

2. Experimental procedure

The a-C:H samples were prepared by deposition from an rf glow discharge plasma of benzene [10]. The deposition conditions (self bias -400 V, pressure 80 mTorr) were such as to yield hard forms of a-C:H samples with a density of $\approx$1.8 g cm^{-3} and hydrogen content of $\approx$35%. For easy removal, an Al plate was used as the substrate.

To characterize the sample, high-resolution CP/MAS ^{13}C spectra [11] at room temperature were measured with proton dipolar decoupling [11] at a proton frequency of 300 MHz and a ^{13}C resonance frequency of 75.47 MHz. The ^{13}C–proton cross-polarization time was 1 ms. The spinning frequency was 4.1 kHz and the total suppression of side bands (TOSS) technique has been used [5]. This technique removes rotational side bands arising from inhomogeneous interactions larger than the spinning frequency. It should be noticed however that because of the use of the proton–carbon cross-polarization technique, non-hydrogenated carbons are not detected here. All ^{13}C chemical shifts are given with respect to tetramethylsilane (TMS). The ^{13}C spectrum clearly showed two pronounced inhomogeneously broadened peaks, one at 124 ppm due to sp^2 carbons and another at $\approx$35 ppm due to sp^3 hybridized carbons. These results are similar to those of other authors [5, 6, 12, 13]. The intensity ratio of the two peaks is about 2.5:1. There is also a

pronounced shoulder centred at 160 ppm. The width of the peak at 124 ppm is about 32 ppm (i.e. ≈2.4 kHz), whereas the weaker peak at 35 ppm is significantly broader (≈3.1 kHz). The rather unusually large width of the two peaks here clearly reflects a distribution of isotropic ^{13}C chemical shifts.

The temperature dependences of the ^{13}C and the ^{1}H magnetization recoveries have been studied using a π–$\pi/2$ pulse sequence. The ^{13}C NMR spectra and spin–lattice relaxation times were measured at a ^{13}C resonance frequency of 95.572 MHz. The ^{1}H spin–lattice magnetization recovery was measured at 100 MHz. Spectrally selective ^{13}C magnetization recovery measurements were performed as well.

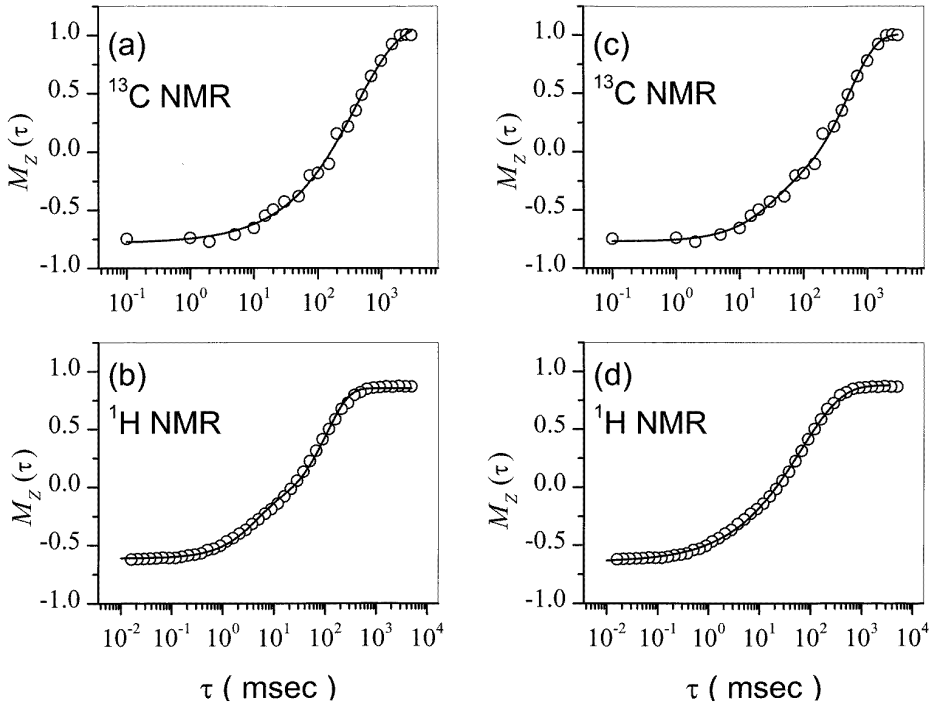

Figure 1. (a) ^{13}C and (b) ^{1}H magnetization recovery curves for an amorphous carbon sample analysed using a two-component relaxation function (equation (1)). (c) ^{13}C and (d) ^{1}H magnetization recovery curves analysed using a stretched-exponential relaxation function (equation (2)).

For the 2D ^{13}C separation-of-interactions experiment, the standard $\pi/2$–$t_1/2$–π–$t_1/2$–echo–t_2 pulse sequence, combined with phase cycling, was used. This technique allows for a separate determination of the ^{13}C spectra with and without inhomogeneous interactions. The ω_1-domain yields the homogeneous ^{13}C lineshapes determined by the ^{13}C dipole–dipole interactions, whereas the ω_2-domain yields the inhomogeneous lineshape determined by the chemical shift contribution and hyperfine interactions between carbons and unpaired electrons.

The X-band electron spin-resonance (ESR) spectra were measured using a Bruker ESP 300E spectrometer equipped with an Oxford cryostat. The d.c. magnetization was measured by a home-built SQUID magnetometer.

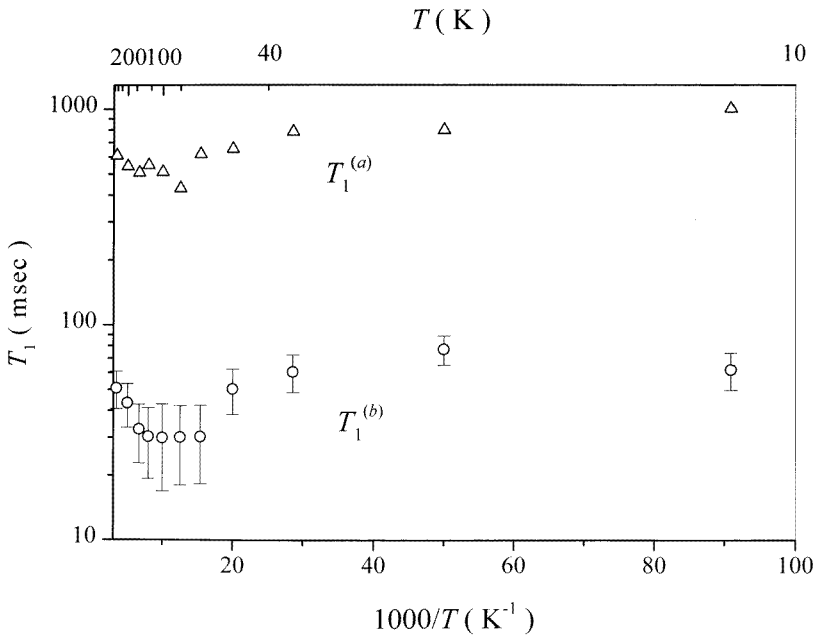

Figure 2. The temperature dependence of the two ^{13}C spin–lattice relaxation time components $T_1^{(a)}$ (△) and $T_1^{(a)}$ (○).

3. Results and discussion

3.1. ^{13}C and ^{1}H spin–lattice relaxation and magnetization recovery

The observed ^{13}C magnetization recovery curves (figure 1(a)) can be fitted within the experimental accuracy by a two-component relaxation function

$$M(t)/M_0 = M_a\left(1 - 2\mathrm{e}^{-t/T_1^{(a)}}\right) + M_b\left(1 - 2\mathrm{e}^{-t/T_1^{(b)}}\right) \tag{1}$$

which is similar to the one reported for the proton (figure 1(b)) magnetization recovery [5, 10]. The relative amplitudes of the two components are $M_a = 0.30$ and $M_b = 0.70$. One component has a ^{13}C T_1-value of the order of $T_1^{(a)} \approx 750$ ms, whereas T_1 for the other component is of the order of $T_1^{(b)} \approx 60$ ms. Both $T_1^{(a)}$ and $T_1^{(a)}$ are nearly temperature independent down to 4.4 K (figure 2). This behaviour is analogous to the bi-exponential relaxation behaviour of the protons, where the two time constants are however shorter by a factor of about 4 (figure 1(b)).

In order to check whether we have a two-cluster region or a multi-cluster region case we tried to fit the observed ^{1}H and ^{13}C magnetization recovery data not only to a bi-exponential but also to a stretched-exponential magnetization recovery function:

$$M(t)/M_0 = 1 - 2\mathrm{e}^{-(t/T_1)^{\alpha}}. \tag{2}$$

The obtained results at room temperature are shown in figures 1(c) and 1(d). The stretched-exponential fits are within the limits of the experimental error actually slightly better that the bi-exponential ones (figure 1(a), 1(b)). The temperature dependences between 100 K and 4 K of the stretch exponent α and the ^{13}C spin–lattice relaxation parameter T_1 are shown in figure 3. In the ^{13}C case, $\alpha = 0.6$, whereas the parameter $T_1(^{13}\mathrm{C})$ is 480 ms. In

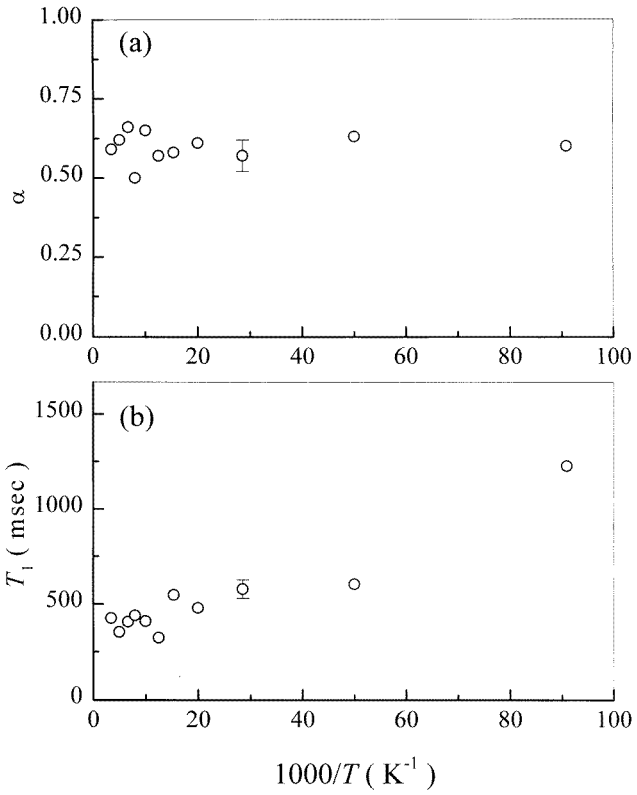

Figure 3. The temperature dependence of (a) the stretch exponent α and (b) the ^{13}C spin–lattice relaxation parameter T_1.

the proton case, we have $\alpha = 0.68$, whereas T_1(H) is 83.5 ms at room temperature. We thus see that within the limit of experimental error the ^{13}C and the ^{1}H magnetization recovery can be described by a stretched-exponential function just as well as by a bi-exponential one.

The observed short values of the ^{13}C spin–lattice relaxation times are in both of the above models hard to understand in terms of the relaxation mechanisms normally operating in non-magnetic polymers and organic solids. C–H dipolar interactions and ^{13}C chemical shift anisotropy relaxation cannot yield such a short ^{13}C T_1-value which would be nearly temperature independent down to 4 K. The same seems to be true for the rather short and temperature independent values of the ^{1}H spin–lattice relaxation time parameters. The only possible mechanism which could yield such a ^{13}C and ^{1}H T_1-behaviour is coupling to paramagnetic centres.

It is well known that in solids the direct electron–nuclear coupling may induce nuclear spin flips unaccompanied by an electron flip. This relaxation mechanism results for $\omega_I \tau \gg 1$ in a nuclear spin–lattice relaxation rate [14]

$$\frac{1}{T_1} = Cr^{-6} \tag{3}$$

where

$$C = \frac{2}{5}\gamma_S^2\gamma_I^2\hbar^2 S(S+1)\frac{\tau}{1+\omega_I^2\tau^2} \tag{4}$$

with τ being the electron spin–lattice relaxation time.

This mechanism is very effective for nuclei close to the paramagnetic centres but rather ineffective for all other nuclei. The majority of the nuclei are in fact relatively far from the paramagnetic centre and are thus relaxed by spin diffusion to paramagnetic impurities. Here [14]

$$\frac{1}{T_1} = 4\pi N b D \tag{5}$$

where N is the number of impurities per unit volume and $D = Wa^2$ is the nuclear spin-diffusion constant with a being an inter-nuclear distance and W the probability of a spin-flop transition between nearest neighbours. b is the scattering amplitude of a single impurity and is of the order of the average inter-nuclear spacing [14].

In the case of spin diffusion, a large number of impurities contribute to spin relaxation at a given lattice site and the magnetization recovery should be described by a single exponential [14]. This is contrary to the bi-exponential behaviour reported in references [5, 10] as well as to the behaviour shown in figure 1.

If however the electrons aggregate into isolated clusters which are preferentially found in some regions of the sample and not in others, we can obtain a multi-exponential magnetization recovery behaviour: we expect a bi-exponential relaxation behaviour if we have two types of region with different values of N. In the case of a continuous distribution of isolated clusters with different values of N, we may even expect a stretched-exponential behaviour. If this electron clustering does indeed occur, one would expect to find a superparamagnetic behaviour at low temperatures. Such a behaviour should show up in the ^{13}C NMR spectra, the ESR spectra and the static magnetic properties at low temperatures.

3.2. Spectrally selective ^{13}C magnetization recovery

An additional check of the above model is provided by spectrally selective ^{13}C T_1-measurements. If the observed ^{13}C T_1-distribution is due to electron clustering, the ^{13}C magnetization recovery should be of the stretched-exponential type within each set of chemically shifted ^{13}C lines. If however the ^{13}C T_1-distribution is due to the presence of two or three ^{13}C species with different chemical shifts, the ^{13}C magnetization recovery should be mono-exponential within each set of chemically shifted ^{13}C lines.

To check on this point we have made spectrally selective ^{13}C magnetization recovery T_1-measurements. For the unprotonated carbons, in particular, spectrally selective measurements were made without ^{13}C–proton cross-polarization and proton dipolar decoupling. The ^{13}C magnetization recovery here cannot be described by a single exponential and clearly shows a stretched-exponential behaviour. At room temperature $T_1(^{13}\mathrm{C}) = 700$ ms and $\alpha = 0.4$. This shows that a T_1-distribution is present already within a given ^{13}C species. It is thus not due to the existence of two or three different sets of ^{13}C lines. This fully supports the proposed model according to which the ^{13}C spin–lattice relaxation is here determined by spin diffusion to paramagnetic impurities and the non-exponential form of the magnetization recovery is due to electron clustering.

3.3. Temperature dependences of the ^{13}C NMR spectra

The ^{13}C NMR powder spectra of our a-C:H samples measured between 290 K and 20 K at 95.572 MHz without MAS and proton decoupling are presented in figure 4. At room temperature the chemical shift anisotropy and dipolar coupling with protons smear out the

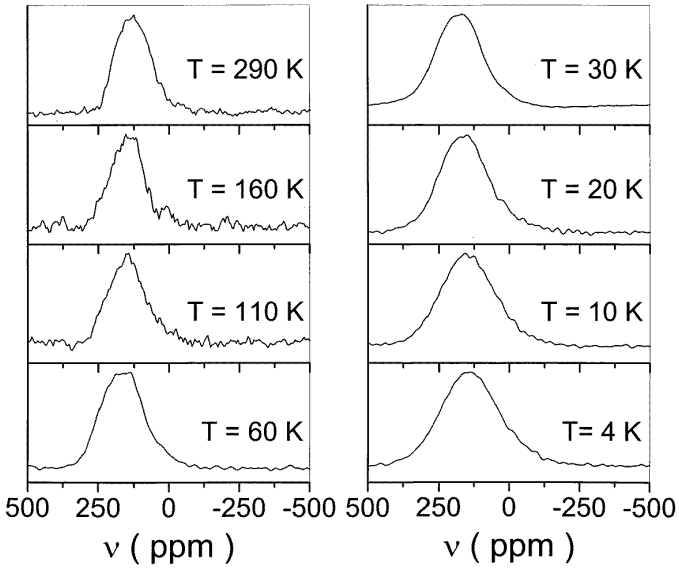

Figure 4. The temperature dependences of the ^{13}C NMR spectra of a-C:H measured at 95.572 MHz.

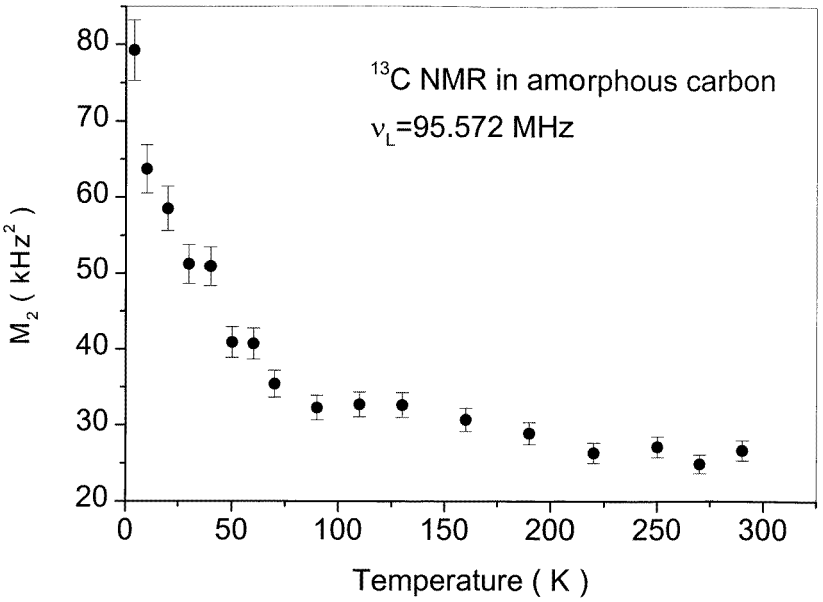

Figure 5. The temperature dependences of the second moment M_2 of the ^{13}C NMR spectra of a-C:H.

two sp^2 and sp^3 carbon peaks, resulting in a broad single unstructured line. At 290 K the width of this inhomogeneous line amounts to ≈15 kHz. A large increase in the width of the ^{13}C spectrum with decreasing temperature is found at low temperatures (figure 4).

The temperature dependence of the second moment M_2 of the ^{13}C NMR spectrum is

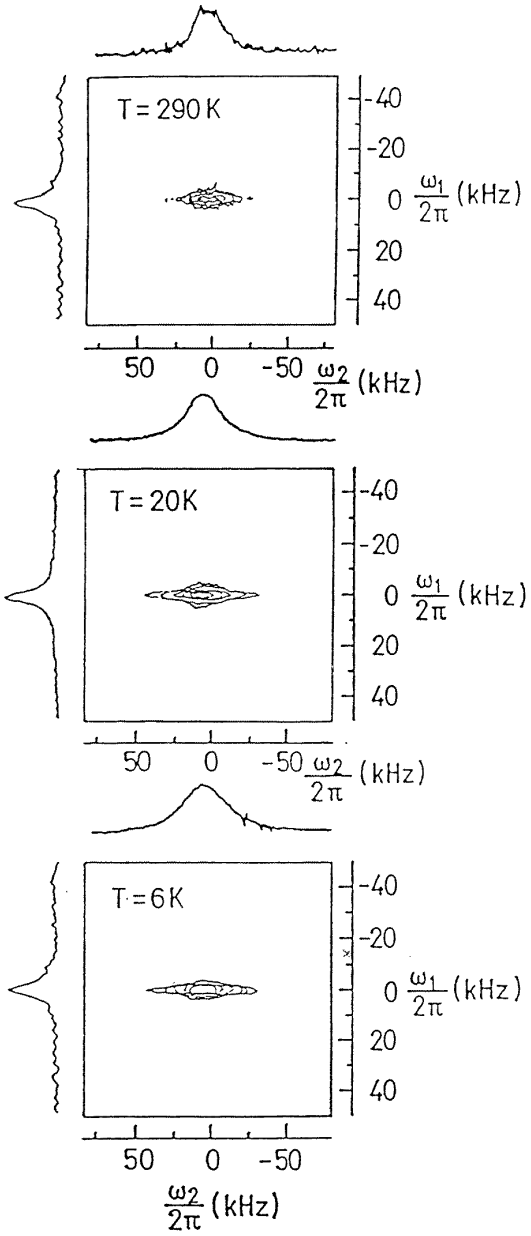

Figure 6. 2D separation-of-interactions ^{13}C NMR spectra of a-C:H.

shown in figure 5. Whereas M_2 is nearly T-independent between room temperature and 70 K—except for a slight increase from 25 kHz^2 to 30 kHz^2 centred at around 150 K—there is a drastic increase in M_2 at low temperatures. M_2 changes from 30 kHz^2 at 70 K to 80 kHz^2 at 4 K.

To see whether the observed increase in the width and the second moment M_2 is due to a freeze-out of molecular motion or due to electron–^{13}C interactions and the increase

of the magnetic susceptibility as expected in the case of superparamagnetic freezing, we decided to measure the 2D separation-of-interactions ^{13}C NMR spectra (figure 6) at different temperatures. At room temperature the ratio between the inhomogeneous and homogeneous (dipolar) widths amounts to 6.6. This ratio increases to 9.55 at 20 K and 11.26 at 6 K. The homogeneous width, 3.33 kHz, is T-independent whereas the inhomogeneous width increases with decreasing temperature and reaches 37.5 kHz at 6 K. This shows that we do indeed deal with ^{13}C–electron interactions and a drastic increase of the magnetic susceptibility. The freeze-out of the hypothetical molecular motion would thus result in an increase of both the homogeneous and the inhomogeneous linewidths. It should also be noted that if the observed increase in M_2 at low temperatures were to be due to a freeze-out of molecular motion, we would find a huge T_1-minimum. This was not observed.

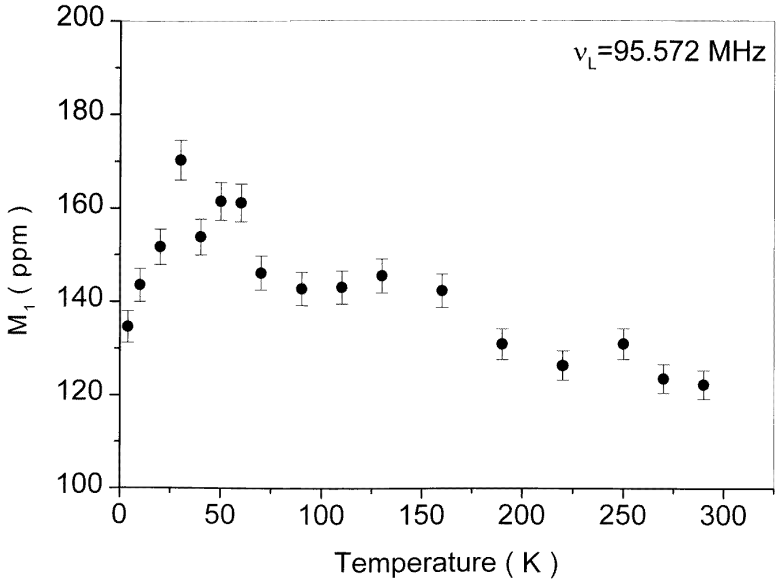

Figure 7. The temperature dependence of the first moment M_1 of the ^{13}C NMR spectra of a-C:H. The first moment is calculated relative to that of TMS.

The centre of the inhomogeneous line shifts with decreasing temperature. The temperature dependence of the first moment M_1 of the ^{13}C line is presented in figure 7. The temperature dependences of M_2 and M_1 both indicate that large changes of the electronic magnetic susceptibility take place below 50 K.

We suppose that the second-moment contributions due to the ^{13}C–proton dipolar interactions H_{dip}(C–H) and the ^{13}C chemical shift tensor contribution H_{CS} are—in the absence of molecular motions—temperature independent and that the temperature dependence of the second moment is due to the electron–^{13}C interactions. If the unpaired electron distribution were to be either completely regular or random, it would be easy to show that the ^{13}C second moment at low temperatures would be proportional to the square of the electron susceptibility. M_2 should in this case increase as the square of the ESR intensity. Since electron clustering occurs, the situation is not so simple and significant deviations from the above prediction can occur. The exact structure and distribution of the paramagnetic clusters are not known at present and a determination of M_2 from first principles is not possible.

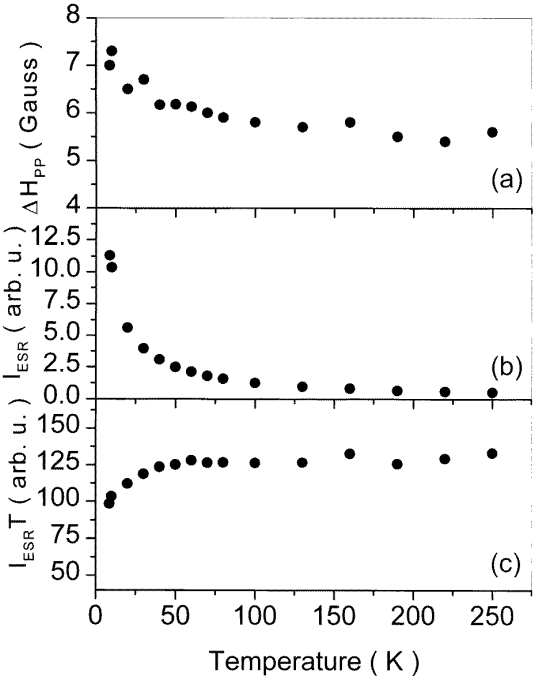

Figure 8. (a) The temperature dependence of the width of the ESR signal of a-C:H. (b) The temperature dependence of the intensity I_{ESR} of the ESR signal a-C:H. (c) The temperature dependence of $I_{ESR}T$ showing the deviation from the Curie law below 50 K.

3.4. ESR spectra

To check on the existence and nature of the paramagnetic centres responsible for the ^{13}C–electron coupling and the anomalous behaviour discussed in sections 3.1 and 3.2, we decided to measure the electron spin-resonance (ESR) spectra. Our a-C:H samples do indeed show a rather strong X-band ESR signal centred at $g = 2.0029$ at room temperature. No other ESR signal has been observed between 0 and 10^4 G. The intensity of the signal corresponds to 2.5×10^{19} free spins g^{-1} for a typical sample. The absence of other ESR lines in the region between 0 and 10^4 G demonstrates that the concentration of other magnetic impurities like iron or chromium is less than 10^{15} spins g^{-1}. The derivative peak-to-peak width of the $g \approx 2$ ESR line is about 6 G at room temperature. Below 25 K the width slightly increases with decreasing temperature and reaches 7.3 G at 6 K (figure 8(a)). The intensity of the ESR line follows the Curie law $I_{ESR} \propto C/T$ down to 50 K (figure 8(b)). Below 50 K the intensity multiplied by the temperature ($I_{ESR}T$) (figure 8(c)) starts to decrease with decreasing temperature. This behaviour again indicates the onset of a superparamagnetic transition (figure 8(c)) due to local freezing of isolated electron spin clusters. The blocking temperature is around 30–40 K.

The above results demonstrate the presence of unpaired electronic spins in our samples. They also show that the short and temperature-independent ^{13}C and ^{1}H T_1-values at low temperatures and the non-exponential magnetization recovery are due to relaxation via paramagnetic centres, aggregating into spatially separated clusters. The same is true for the increase in the inhomogeneous width of the ^{13}C NMR spectra at low temperatures.

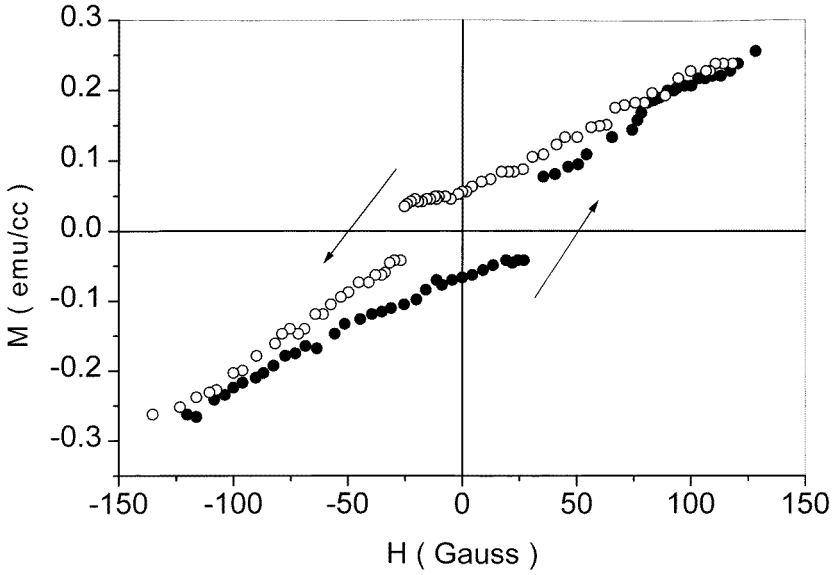

Figure 9. The magnetic hysteresis loop measured by a SQUID magnetometer for a-C:H at 4.2 K.

3.5. Magnetic hysteresis loop measurements

The anomalous magnetic behaviour of our samples of amorphous hydrogenated carbon at low temperatures is confirmed by the observation of a distinct magnetic hysteresis loop in a field of −150 to +150 G (figure 9) and a residual magnetization obtained by SQUID measurements at 4.2 K. The hysteresis loop is similar to the one observed for other superparamagnets [15] and is due to the time lag between the change in the external magnetic field and the response of the magnetization. A hysteresis loop has also been observed at 20 K, the highest temperature which can be reached with our present SQUID magnetometer.

4. Conclusions

From the above results the following conclusions can be drawn.

(a) The short and nearly temperature-independent values of both the proton and the ^{13}C spin–lattice relaxation times demonstrate that the dominant spin–lattice relaxation mechanism is spin diffusion to paramagnetic impurities. The fact that the magnetization recovery is not described by a single exponential as expected in the case of a random distribution of paramagnetic centres but shows a bi-exponential or stretched-exponential form further demonstrates that the paramagnetic centres aggregate into isolated clusters, leading to superparamagnetic behaviour at low temperatures.

(b) The temperature dependence of the inhomogeneous widths of the ^{13}C NMR spectra obtained by 2D ‘separation-of-interactions’ techniques demonstrates that the measured a-C:H sample is indeed heterogeneous on a microscopic scale. The large increase in the inhomogeneous width at low temperatures is the result of ^{13}C–electron coupling and the increase in the magnetic susceptibility expected for the case of superparamagnetic freezing.

(c) The increase in the second moment of the inhomogeneous ^{13}C NMR frequency distribution with decreasing temperature and the temperature shift of the centre of the ^{13}C NMR spectra are also indicative of electron–^{13}C interactions and superparamagnetic freezing.

(d) The observed g-factor in the ESR spectra, which is close to the free-electron value, demonstrates that unpaired free electrons are present in amorphous hydrogenated carbon rather than magnetic (e.g. Fe) impurities.

(e) The observed concentration of unpaired electrons, 2.5×10^{19} electrons per gram, in a typical sample means that we have about one unpaired electron per 2400 atoms. If the distribution of electrons were to be homogeneous, this would mean that the mean inter-electron separation is about 56 Å. Such a distance is much too large to allow for the occurrence of a magnetic anomaly induced by exchange interactions. The observed magnetic anomalies below 50 K thus do indeed show that the spatial distribution of unpaired electrons is not homogeneous, as already concluded from the ^{1}H and ^{13}C spin–lattice relaxation magnetization recovery results. The observed deviation of the ESR intensity from the Curie law below 50 K is also indicative of a freezing of superparamagnetic clusters.

(f) The observed magnetic hysteresis at low temperatures seems to be the result of the time delay between the change of the external magnetic field and the response of the system. Such a behaviour is indeed known to occur in superparamagnets containing a macroscopically large number of well isolated, nearly identical magnetic moments [15–17].

Acknowledgment

The work of IP and MK was supported by the Hungarian Science Foundation under contract numbers OTKA-T-4223 and OTKA-T-017371

References

[1] Robertson J 1986 *Adv. Phys.* **35** 317
Robertson J 1991 *J. Non-Cryst. Solids* **137+138** 825
[2] Robertson J 1991 *Prog. Solid State Chem.* **21** 199
[3] Walters K, Honeybone P J R, Huxley D W and Newport R J 1994 *Phys. Rev.* B **50** 831
[4] Honeybone P J R, Newport R J, Walters J K, Howells W S and Tomkinson J 1994 *Phys. Rev.* B **50** 839
[5] Jäger C, Sottwald J, Spiess H W and Newport R J 1994 *Phys. Rev.* B **50** 846 and references therein
[6] Carduner K R, Rokosz M J, Tamor M A and Vassell W C 1991 *Appl. Magn. Reson.* **2** 647
[7] Walters J K, Rigden J S, Newport R J, Parker S F and Howells W S 1995 *Phys. Scr.* T **57** 142
[8] Mauri F, Pfrommer B G and Louie S G 1997 *Phys. Rev. Lett.* **79** 2340
[9] Jäger C, Titman J J and Newport R J 1993 *Thin Solid Films* **225** 3
[10] Pocsik I, Koos M, Moustafa S H, Lasanda S, Banki P and Tompa K 1996 *J. Non-Cryst. Solids* **198–200** 632
[11] Mehring M 1983 *Principles of High Resolution NMR in Solids* (Berlin: Springer)
[12] Jansen F, Machonkin M, Kaplan S and Hark S 1985 *J. Vac. Sci. Technol.* A **3** 605
[13] Pan H, Pruski M, Gerstein B C, Li F and Lannin J S 1991 *Phys. Rev.* B **44** 6741
[14] Abragam A 1960 *The Principles of Nuclear Magnetism* (Oxford: Oxford University Press)
[15] Gatteschi D, Caneschi A, Pardi L and Sessoli R 1994 *Science* **265** 1054
[16] Dobrovitski V V and Zvezdin A K 1997 *Europhys. Lett.* **38** 377
[17] Barbara B, Wernsdorfer W, Sampaio L C, Park J G, Paulsen C, Novak M A, Ferre R, Mailly D, Sessoli R, Caneschi A, Hasselbach K, Benoit A and Thomas L 1995 *J. Magn. Magn. Mater.* **140–144** 1825